# Domain Structures in Low Ionic Strength Polyelectrolyte Solutions

**Brett D. Ermi and Eric J. Amis***

*Polymers Division, National Institute of Standards and Technology, Gaithersburg, Maryland 20899*

*Received April 14, 1998; Revised Manuscript Received August 21, 1998*

ABSTRACT: A steep upturn at low angles dominates the small-angle neutron scattering profile of low ionic strength polyelectrolyte solutions. This behavior is demonstrated for poly(*N*-methyl-2-vinylpyridinium chloride) in $D_2O$ by measurements that are extended to low angles not typical of most studies. This behavior is consistent with static and dynamic light scattering measurements performed on the same solutions. Specifically, the upturn at low $q$ and the slow diffusive mode in dynamic light scattering indicate the presence of supramolecular structures, which we interpret as large domains of increased polymer concentration. In these same solutions, a shorter wavelength correlation is evident from the presence of a maximum at finite $q$ in the small-angle scattering experiment. Fluctuations on a short wavelength are also apparent from the existence of the fast mode in the dynamic light scattering. The maximum is interpreted as reflecting a characteristic dimension defined by order within domains, while the fast mode results from electrodynamic coupling of fast moving counterions and portions of chains.

## Introduction

Scattering methods have developed into powerful tools for the characterization of polymers.[1−4] Numerous theories and experiments have proven the methods invaluable to understanding the fundamental physics and properties of a wide range of systems, especially neutral polymer solutions. For polyelectrolyte solutions containing excess low-molecular-weight salt, dynamic light scattering (DLS), static light scattering (SLS), and small-angle neutron scattering (SANS) have been used in the same way as for neutral polymer solutions.[4] The well-developed models for interpreting scattering data from neutral polymers can be applied, and parameters such as molecular weight, size, and shape can be readily attained. However, if the ionic strength of the solution is reduced, the observed behavior is altered dramatically and interpretation of the scattering data is not straightforward. These observations have been attributed to the presence of strong, long-range Coulombic interactions, which are coupled to the already complicated behavior of macromolecular solutions. So-called polyelectrolyte effects result, and they disrupt all methods of characterization. Although polyelectrolyte effects are now considered universal for charged macromolecular systems and decades of research have focused on understanding the fundamental physics, polyelectrolytes "remain among the least understood systems in macromolecular science".[5]

DLS from low ionic strength polyelectrolyte solutions displays two relaxations, one an order of magnitude faster and one at least an order of magnitude slower than the single-chain value. Over the past 2 decades these general effects have been reported for nearly all classes of charged macromolecular systems, including biological polyelectrolytes,[6−10] weakly and highly charged synthetic polyelectrolytes in aqueous and nonaqueous solutions,[11−19] and spherical polyelectrolyte dendrimers.[20] The fast mode has been attributed to coupled diffusion of polyions and low-molecular-weight counterions,[6,9−11,21] propagation of excitations in a polyelectrolyte pseudolattice,[7] or thermally excited displacements of polymer segments between entanglements.[13] The slow mode has been interpreted as representing supramolecular structures,[6−8,13−17,21] as evidence of a reptation mechanism,[11] or as impeded diffusion in a congested solution.[13] A further complexity is that recent experiments have shown that under certain conditions a third mode is observed, which is intermediate in value between the fast and slow modes.[18,19]

In small-angle scattering of polymer solutions, the angular and concentration dependence of the time-averaged scattered intensity is measured. This allows determination of molecular weight, radius of gyration, and second virial coefficient.[1,4] For neutral polymer and for polyelectrolyte solutions with added salt, this analysis is possible because these systems are free from long-range interactions or order which results in scattering profiles that are monotonically decreasing functions of angle. However, SAXS and SANS from polyelectrolyte solutions show a broad maximum in the angular dependence of the scattered intensity, whose position is a strong function of polymer concentration. Similar to the two modes in the DLS, this effect has been reported for nearly all types of charged macromolecules, including biological systems,[10,22−24] low- and high-charge density synthetic systems in aqueous and nonaqueous solutions,[15,25−35] and charged dendritic polymer systems.[36−38] This polyelectrolyte maximum has been interpreted within models of a correlation hole,[39,40] scaling theory,[15,33,34,41−43] microphase separation of hydrophobic domains,[30,32] order among highly stretched or cylindrical polyelectrolytes,[22,24,26] and order among polyelectrolytes in a "two-state structure".[29] Some of these models have been combined in various permutations.

Many groups have also observed a sharp upturn at very low scattering angles,[15,23−28,31,32,34−38] demonstrating the presence of long-wavelength concentration fluctuations. Interpretation of this upturn has received very little attention in the literature. It appears at values of $q$ below 0.02 Å$^{-1}$, where $q$ is the scattering wavevector whose magnitude is defined as $q = (4\pi/\lambda_0)\sin(\theta/2)$, with $\lambda_0$ the radiation wavelength and $\theta$ the scattering angle. Because most SANS and SAXS data reported do not extend to values of $q$ much below 0.01 Å$^{-1}$, it has been difficult to quantify the low-angle data. Additionally, with the number of data points being few,

10.1021/ma980579+ 
Published on Web 10/02/1998

some investigators have ignored the data or dismissed it as an artifact or as insignificant.

In one SANS investigation on poly(styrene sulfonate)/$D_2O$ solutions by Ise and co-workers,[28] the $q$ range was extended to lower values, and indeed the upturn dominated the scattering profile. The low-angle data were analyzed using the Guinier method with reported $R_g$ values ranging from 40 to 70 nm. Although the fits to the data were imperfect and the authors admitted the quantitative results were questionable, these measurements demonstrate that the upturn contributes substantially to the overall scattering. One of the difficulties for interpreting polyelectrolyte scattering data has been that few investigations combine static light scattering and neutron scattering with dynamic light scattering on the same samples.

A recent study of a well-defined DNA fragment by Borsali et al.[10] is an exception and suggests the power of such an approach. In their study the neutron scattering showed the finite $q$ maximum of scattering intensity as well as the upturn at low $q$. Separate static and dynamic light scattering measurements were also analyzed as shown previously. However, the $q$ ranges were not comparable so the data could not be compared quantitatively. The study demonstrates clearly that for polyelectrolyte systems a complete investigation of static scattering over a broad $q$ range is required.

In the current study, we provide such data with a complete picture of the static scattering for a well-defined polyelectrolyte system by a qualitative combination of SLS and SANS over an extended $q$ range. Specifically, SANS experiments on poly($N$-methyl-2-vinylpyridinium chloride) (PMVP) in deuterium oxide cover 2 orders of magnitude in $q$ values and extend to $q$ values at least a factor of 6 lower than typical experiments. In addition, we present static light scattering from the same PMVP solutions to extend the $q$ range to even lower values. For studying the dynamics of these solutions, DLS measurements are also presented.

## Experimental Section

Poly($N$-methyl-2-vinylpyridinium chloride) preparation has been described previously.[17,44] Briefly, anionically polymerized poly(2-vinylpyridine) ($M_w = 281\,000$; $M_w/M_n = 1.03$)[45] obtained from Pressure Chemical[46] was quaternized with dimethyl sulfate in dimethylformamide solution at room temperature. The crude polyelectrolyte was dialyzed, counterion-exchanged, and lyophilized to obtain the dry chloride salt. The degree of quaternization of the polymer used in this study was 70% as measured by standard counterion titration. Solutions were prepared with $D_2O$ from dry PMVP and transferred to quartz scattering cells for SANS measurements. Following these measurements, the solutions were filtered through 0.20-$\mu$m Millipore membrane filters directly into sealable, dust-free cells for light scattering measurements. Deuterium oxide ($D_2O$; Cambridge Isotopes, 99.9% D, low paramagnetic) was used as received.

Static and dynamic light scattering measurements were performed with a Brookhaven (BI-200SM) light scattering goniometer using an Ar ion laser (Spectra Physics 2020-3) operating at 488 nm as the light source. Static light scattering measurements were performed over an angular range of 25−145° at 2° intervals. Photon autocorrelation functions were acquired with a log time digital correlator (ALV-5000) over an angular range of 35−145°. The correlation curves were analyzed using CONTIN, the inverse Laplace transform program of Provencher.[47,48]

Small-angle neutron scattering measurements were performed on the 30-m SANS instrument of the Cold Neutron Research Facility at the National Institute of Standards and Technology. The neutron beam was monochromated to 9 Å with a velocity selector having a wavelength spread of 0.25 ($\Delta\lambda/\lambda = 0.25$). The scattered neutrons were detected by a 64-cm × 64-cm two-dimensional detector using two different sample-to-detector distances, 15.3 and 2.0 m. These configurations allow values of the scattering wavevector $q$ in the range $0.0025 < q$ (Å$^{-1}$) $< 0.024$ and $0.016 < q$ (Å$^{-1}$) $< 0.17$, respectively. Here $q$ is the scattering vector defined as $q = (4\pi/\lambda_0)\sin(\theta/2)$, with $\lambda_0$ the neutron wavelength (9 Å) and $\theta$ the scattering angle. The resulting data were corrected for background electronic noise, detector inhomogeneity, empty cell scattering, and solvent scattering. Following correction for sample transmission, the intensities were scaled to absolute values using a polymer standard for the 15.3-m configuration and a silica standard for the 2.0-m configuration. The uncertainties of the individual data points for the $I(q)$ versus $q$ plots are calculated statistically from the number of averaged detector counts. For the plots displayed in this publication, the relative standard uncertainties are less than ±2% of the intensity values and are not shown.[49]

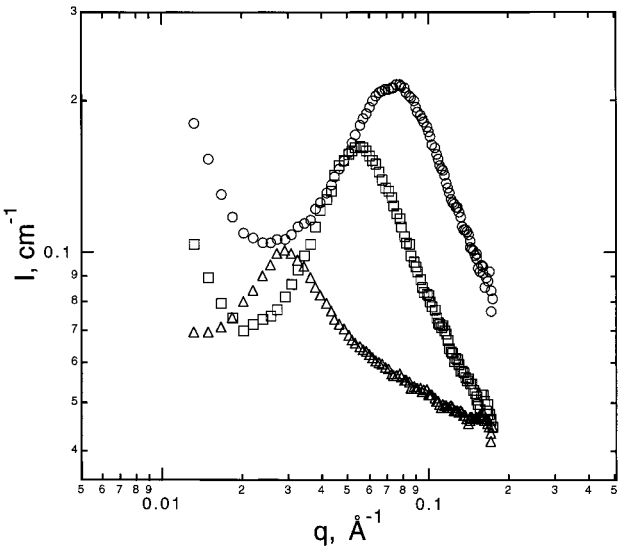


**Figure 1.** Log−log plot of SANS scattered intensity, $I(q)$, plotted versus the scattering vector $q$ for PMVP in $D_2O$ for three polymer concentrations: (△) 3.0 g/L, (□) 15 g/L, and (○) 30 g/L using an instrument configuration which provides a $q$ range typical of previous measurements.

## Results

Figure 1 displays the SANS profiles of PMVP in $D_2O$ with no added salt for concentrations ranging from 3.0 to 30 g/L on a log−log plot using an instrument configuration which measures $q$ values in the range $0.016 < q$ (Å$^{-1}$) $< 0.17$, a range typical of previous investigations. Each curve shows one broad maximum whose position is a strong function of concentration, moving to higher $q$ with increasing concentration. At $q$ values below 0.02 Å$^{-1}$, a sharp upturn is evident in the curves for the 30 and 15 g/L samples but is not observed for the 3.0 g/L sample.

We extended our measurements to $q$ values not typical for SANS on polyelectrolyte solutions by using a second, longer sample-to-detector distance. This configuration allows us to probe $q$ values in the range $0.0025 < q$ (Å$^{-1}$) $< 0.024$. Figure 2 shows the scattering profiles for the two separate instrument configurations plotted together in log−log format for the same three $D_2O$ solutions of PMVP. Effectively, this figure extends the data in Figure 1 to lower $q$ values by a factor of 6 for a more complete description of the static structure. Figure 2 demonstrates that the low-angle upturn domi-

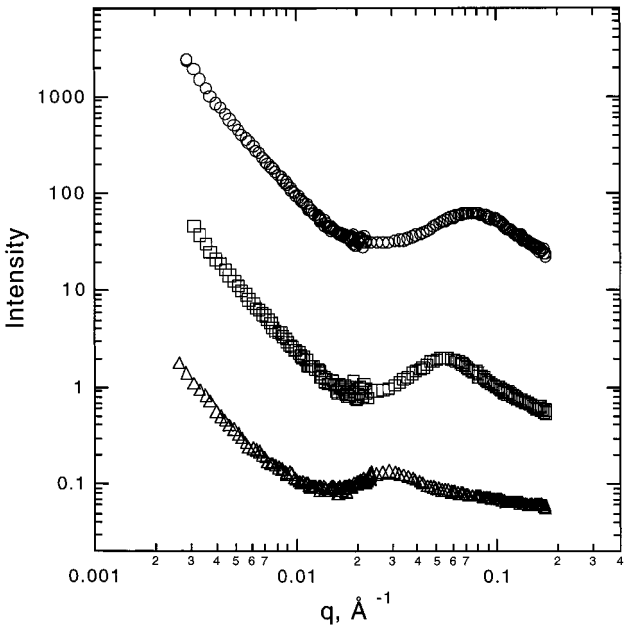


**Figure 2.** Log−log plot of SANS scattered intensity, $I(q)$, plotted versus the scattering vector $q$ for PMVP in $D_2O$ for three polymer concentrations: (△) 3.0 g/L, (□) 15 g/L, and (○) 30 g/L using two separate configurations. The first configuration is identical to Figure 1, while the second provides $q$ values over a factor of 6 smaller. For clarity of presentation the 15 and 30 g/L data have been shifted up by 1 and 2 decades, respectively.

nates the overall scattering, and it can be considered neither insignificant nor an artifact. Note that the intensities from the two different configurations are in absolute intensity units. To match the data in the overlapping $q$ range, no arbitrary adjustments of intensities were required, and the consistency of the data for each sample from the two configurations is excellent. For each concentration the curves are qualitatively the same: a broad maximum at high $q$, with the steep upturn now a dominant feature in the scattering covering almost an order of magnitude in $q$. The sharp decrease in scattering intensity with increasing $q$ follows an apparent power law, $I(q) \propto q^{-2.2\pm0.2}$, for each sample.

Figure 3 displays the normalized light scattering intensity, $I(q)/I(0)$, where $I(q)$ is the excess scattering intensity at wavevector $q$, on a log−log plot for PMVP in $D_2O$. These SLS measurements were performed on the same solutions as used for the SANS experiments, except the samples were filtered properly into light scattering ampules prior to the measurements. Also shown in Figure 4 are Debye function fits to the data according to the formula,

$$I(q) = A + \left(\frac{B}{x^2}\right)(e^{-x} - 1 + x) \qquad (1)$$

where $x = q^2\langle R_g^2\rangle$, $R_g^2$ is the mean square radius of gyration, $A$ is an incoherent baseline parameter, and $B$ is an intensity scaling factor. The results of nonlinear curve fitting for $R_g$ are displayed in Table 1. The Debye function fits the data well over a wide range of scattering angles for each concentration. $R_g$ is virtually independent of concentration, and the values of 90 nm are comparable to those obtained in previous studies.[13,16]

It is possible to combine data from the light and neutron static scattering covering these different but overlapping $q$ ranges. Figure 4 shows such a plot. For

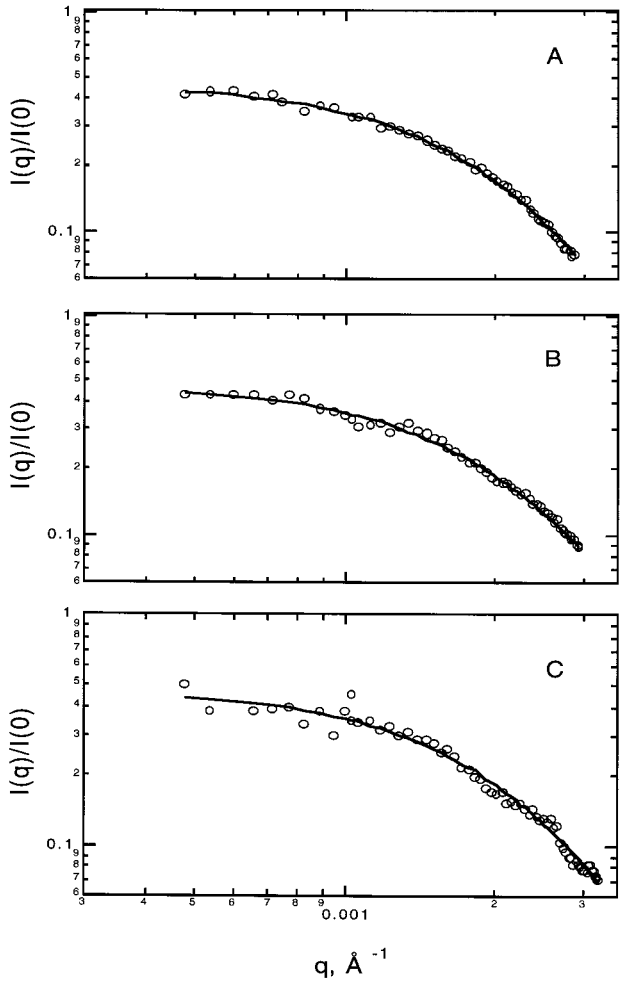


**Figure 3.** Log−log plot of SLS scattered intensity for PMVP in $D_2O$ for three polymer concentrations: (A) 30 g/L, (B) 15 g/L, and (C) 3.0 g/L. The solid lines are Debye functions fit to the data with the results given in Table 1.

this figure the light scattering intensity at each $q$ value was adjusted by a constant factor so that the SLS data overlap with the SANS data in the region of comparable $q$. The scattering profiles now cover a $q$ range of nearly 3 decades. The curves from light scattering and neutron scattering are consistent for each of the concentrations investigated. For clarity of presentation the 15 and 30 g/L data have been shifted up by 1 and 2 full decades, respectively.

As mentioned earlier, numerous investigators have observed two diffusive relaxations by dynamic light scattering for low ionic strength polyelectrolytes in water. To complete the picture of the scattering results, dynamic light scattering was performed on these solutions. As expected, DLS for our polyelectrolyte in deuterated water shows the same qualitative features. Figure 5 shows a representative correlation function for PMVP in $D_2O$ covering 8 decades of time together with the spectrum of characteristic relaxation times obtained by CONTIN. The fast and slow relaxations times, $\tau_f$ and $\tau_s$, respectively, are separated by more than 3 decades and are easily resolved. This behavior is typical of DLS from low ionic strength polyelectrolyte solutions.

## Discussion

Light and neutron scattering provide complementary measurements of the same physical phenomenon of

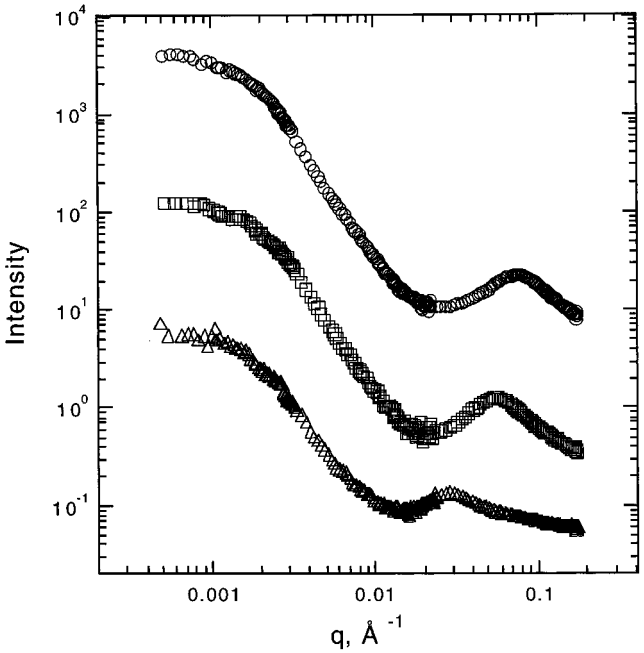


**Figure 4.** Log−log plot of SANS scattered intensity and SLS scattered intensity, $I(q)$, plotted versus the scattering vector $q$ for PMVP in $D_2O$ for three polymer concentrations: (△) 3.0 g/L, (□) 15 g/L, and (○) 30 g/L. Each set of SLS data has been shifted vertically to match the SANS data. For clarity of presentation the 15 and 30 g/L data have been shifted up by 1 and 2 decades, respectively.

**Table 1. Values of Radius of Gyration Extracted from Debye Function Fits to SLS from PMVP in $D_2O$[a]**

| concentration, g/L | $R_g$, nm |
|---|---|
| 3.0 | 88 ± 2.0 |
| 15 | 89 ± 1.7 |
| 30 | 93 ± 1.7 |

[a] ± Values are the standard uncertainty.

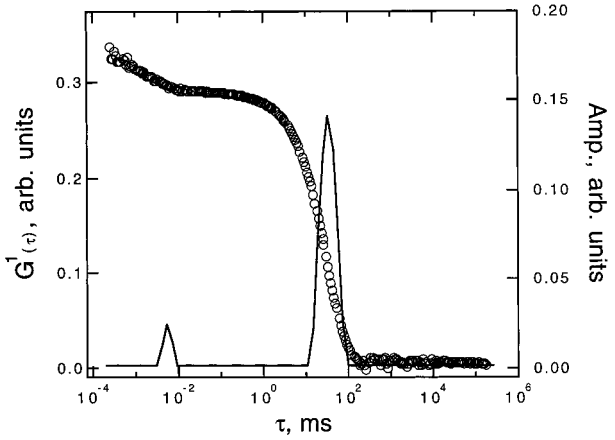


**Figure 5.** Representative dynamic light scattering correlation function for PMVP in $D_2O$ showing two widely separated relaxations. The solid line is the spectrum of relaxation times obtained by CONTIN analysis: $\theta = 45°$, $c_p = 30$ g/L.

concentration fluctuations in polymer solutions.[50,51] Except for the differences in cross sections seen by neutrons and light, the two techniques differ only in the radiation wavelength so that scattering by light probes low wavevector values, where large-scale fluctuations dominate, and SANS probes relatively higher wavevector values, where short-wavelength fluctuations dominate. In a general sense, $1/q$ may be thought of as the "magnification level" or "spatial resolution" of the scattering experiment so that light scattering is more sensitive to large scatterers and neutron scattering is more sensitive to small scatterers.

The static, time-averaged scattering intensity $I(q)$ measured as function of scattering wavevector is related directly to the Fourier transform of the density−density correlation function and therefore contains all of the structural information. Because this information is measured in reciprocal space and the scattering contains contributions from both intra- and interchain correlations, data interpretation relies on assuming explicit structural models in real space and subsequently a self-consistent analysis in Fourier space. For most treatments it is assumed that the intraparticle scattering form factor $P(q)$ and the solution structure factor $S(q)$ combine in $I(q)$ as

$$I(q) = KcP(q)S(q) \tag{2}$$

where $K$ is a contrast factor and $c$ is the mass concentration. Typically, individual contributions from the form factor and structure factor can be separated because $P(q)$ is normalized to 1 at small $qR_g$ and $S(q)$ goes to 1 at high $q$ for systems without long-range intermolecular order. In practice this is accomplished by measuring either the light or neutron scattering from dilute polymer solutions, where intermolecular effects are diminished so the scattering is assumed to arise from isolated, noninteracting chains (i.e., $I(q) \approx P(q)$). For dilute polyelectrolyte solutions this approach fails because the shape of the scattering curve is determined by scattering events occurring on multiple length scales. Extrapolation to dilute solution does not guarantee a clean separation of $P(q)$ because of long-range interactions which give nonzero values of $S(q) - 1$ at finite $q$ values. In this case, the combination and overlap of light and neutron scattering expand the window of scattering space so that it may be possible to cover the full relevant $q$ range for both $P(q)$ and $S(q)$. The combined data provide the best test with which to evaluate the various models that have been proposed to describe scattering from polyelectrolyte solutions.

Most models for polyelectrolytes are extensions of scaling theories for neutral polymers. For example, the isotropic model introduced by de Gennes et al.[41] distinguishes three concentration regimes and assumes that strong intramolecular interactions in polyelectrolytes are screened by increasing polymer concentration. In dilute solutions, the polyions are on average widely separated and highly stretched, with overall polyion size being a linear function of the degree of polymerization. Above a certain but still relatively low concentration, the chains can no longer orient freely, and they build up a three-dimensional periodic lattice. At higher concentrations when the chains overlap considerably, a transient network forms similar to the case of neutral entangled polymer solutions. For distances beyond a correlation length $\xi$, electrostatic interactions are screened by the presence of other polyions and counterions, while at distances shorter than $\xi$, electrostatic interactions are significant and the chains behave as rigid segments. At large distances, the polyion can be considered a random walk of segments whose statistical length is on the order of $\xi$. A peak in $S(q)$ is predicted whose position depends on the square root of polymer concentration. Although this isotropic model describes adequately the peak in the scattering, it does not predict the excess low $q$ scattering.

One the other hand, for weakly charged aqueous polyelectrolyte solutions, it has been predicted that competition between the hydrophobic nature of the chain backbone and the electrolyte nature of the charged monomers may lead to stable mesophases under certain experimental conditions.[52,53] Following this interpretation, the maximum represents the characteristic length scale of the microphase-separated polymer-rich hydrophobic domains and polymer-poor hydrophilic domains. This model was not intended for high-charge density systems, nor is it sufficient in a generic sense as was demonstrated recently in our experiments using a polymer−solvent system without backbone hydrophobic interactions,[17,35] which still show the two diffusive modes, polyelectrolyte maximum, and upturn at low $q$. Although it is likely poor solvation of the chain backbone affects the overall physics of polyelectrolyte solutions, especially for low-charge density systems, our previous work demonstrates that these effects are unnecessary to produce the behavior typical of polyelectrolyte scattering.

Previous studies have related the low $q$ static scattering to the slow diffusive mode in DLS.[15,16] The slow mode scattering is attributed to diffusive relaxation of cooperative multichain fluctuations or domains. This mode is diffusive which implies that dissipation of multichain structures is a random process but not necessarily that discrete bundles of chains are experiencing random diffusion. For poly(styrene sulfonate) solutions in water, the domain sizes were determined by SLS to be between 60 and 100 nm, relatively independent of molecular weight over the range 5 000−1 200 000 g/mol.[16] These observations are consistent with the results in Table 1 and Figure 5 from PMVP in $D_2O$. As we have shown, the upturn at low angles in the neutron scattering is also consistent with these measurements of large-scale domains in SLS. This can be seen most clearly in Figure 4 in which the light scattering data are adjusted so that their intensity values are equal in the overlap region with SANS data. Such a comparison is possible because we have covered a sufficient data range to demonstrate that the shape of the low $q$ data is consistent in the region where SLS and SANS overlap. Previous studies have not made such a comparison.[10,15] The low $q$ data can be interpreted as arising from the intraparticle scattering function, $P(q)$, of multichain domains possessing a characteristic radius of gyration of 90 nm.

Schematically, the polyelectrolyte domains might appear as in Figure 6 where the chain density within multichain domains increases with concentration while their overall size remains invariant. The independence of the domain size on concentration and molecular weight is the single most compelling evidence that domains arise from electrostatic interactions which do not depend on the specifics of chain dimension and conformation. We note that this interpretation follows the spirit of the semidilute polyelectrolyte solution model of Muthukumar[54] which predicts an effective attractive interaction between similarly charged polyion segments. Indeed several other recent models have suggested that there is a region of attractive potential generated by purely electrostatic interactions which could lead to cooperativity between macroions in solutions.[55−60] To our knowledge none of these models provide estimates of the range of cooperativity that would suggest a finite domain size, and several of the models rely on a rigid or rodlike polyion conformation.

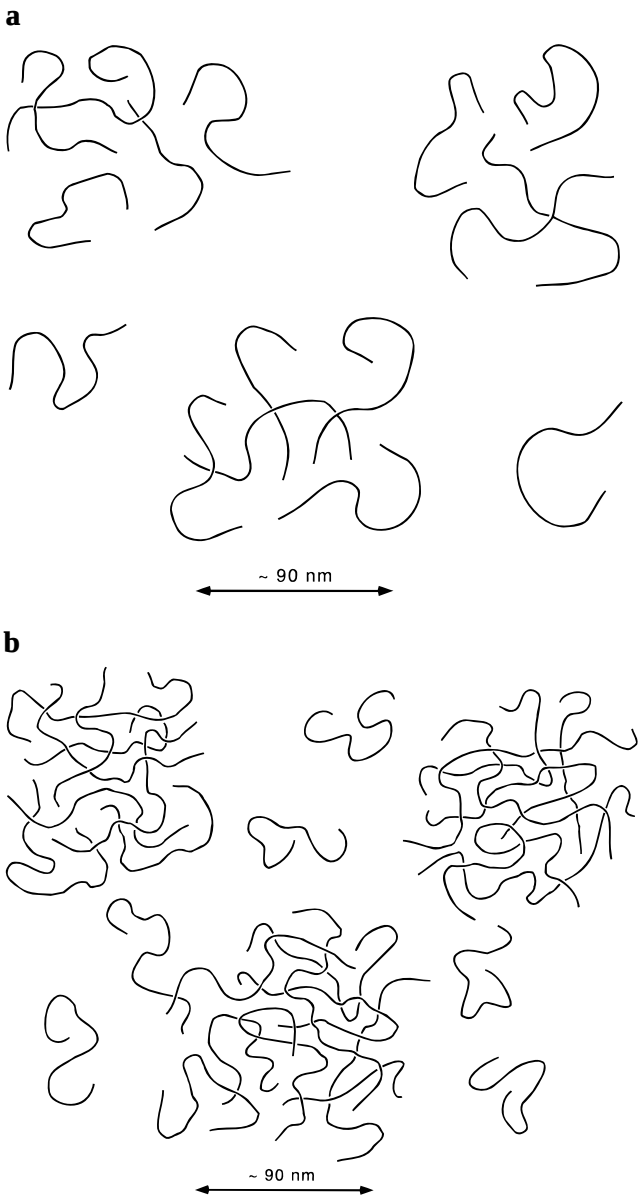


**Figure 6.** Schematic two-dimensional representation of polyelectrolyte domains in relatively dilute and relatively concentrated solutions. Note that with increasing concentration the overall domain size remains constant, while the relative monomer density within domains changes.

In dynamic light scattering the domains give rise to the slow diffusional mode, and likewise we may wish to make a comparison between the fast mode in DLS and the broad maximum in SANS which corresponds to the smaller length scale. Although both techniques suggest a second shorter length scale is important, there are notable differences in the phenomenology. The position of the SANS peak shows strong concentration dependence, while the DLS fast mode is known to be independent of concentration over the same range.[16] In previous studies, the fast mode appears for short chains (5 000 MW) as well as long chains (1 000 000 MW) and in solutions that range from dilute to concentrated.[16] Over more than a decade in concentration at the high end, $D_f$ is independent of molecular weight. Clearly, the fast relaxation cannot reflect accelerated diffusion of entire polyions. The length scale of polyion−counterion

coupling must encompass only a finite portion of the macroion. In such a scenario, counterion fluctuations dominate the dynamics, overwhelming the hydrodynamic contributions.[21] Under this interpretation, the fast mode can be relatively insensitive to the overall structure of the polyelectrolyte solution (i.e., to polymer concentration and molecular weight), as is observed experimentally.[16] Since the static structure factor is the intermediate dynamic structure factor $S(q,\tau)$ as $\tau \rightarrow 0$, any part of the static structure factor has dynamics associated with it and vice versa. It is possible for the concentration dependence of $q_{max}$ and $\tau_c$ to be different even if they have the same physical origin. However, to define their relationship it will be necessary to measure the structure and dynamics in the same $q$ range, for example, by comparing neutron spin−echo and SANS measurements. Nevertheless, that the polyelectrolyte fast mode represents the coupling of fast moving counterions and segments of polyions is consistent with an isotropic model.

The isotropic model seems to correctly predict the $c_p^{0.5}$ scaling of the peak position which has been verified by several investigations. However, this $c_p^{0.5}$ scaling is derived specifically for solutions which are homogeneous throughout. Our results suggest an alternative in which the constraint that the solution be isotropic throughout is relaxed while still requiring the solution to be homogeneous over the finite size defined by the large-scale domains. Within each domain, several chains produce an entangled network that extends throughout that domain. As in the isotropic model, the short-range order among segments of polyions gives rise to a peak in the interparticle structure factor $S(q)$. However, the $c_p^{0.5}$ scaling of the "mesh size" seems to require that the macroions are distributed among domains of fixed volume fraction and number. It is not obvious why this requirement would be met, but it is consistent with the data in Table 1 which demonstrates that for an order of magnitude change in concentration the size of the domains does not change.

Our interpretation is conceptually similar in some respects to the model proposed by Förster et al.[15] Their original model assumed that a polyelectrolyte solution is an isotropic entangled network, with temporal domains of enriched polymer concentration forming in random places within the otherwise homogeneous network. This viewpoint is certainly reasonable for most high-molecular-weight and more concentrated low-molecular-weight solutions. However, the presence of the slow mode in dilute solutions of 5 000 MW poly(styrene sulfonate)[16] would indicate that domains are present even in dilute polyelectrolyte solutions. In our view, it is not necessary for the solution to be an entangled network before multichain domains form. Furthermore, Förster et al. relate the fast mode to a gel mode in a transient network, whereas we attribute the fast mode to electrodynamic coupling of chain segments and fast moving counterions. This reinterpretation of the literature data and the data in ref 15 was later adopted by Förster and Schmidt in a review article.[61] We believe it is now clear that these experimental observations, described as "polyelectrolyte effects", are nearly universal in their appearance. For molecular systems ranging from linear polyelectrolytes to globular proteins to DNA fragments to spherical dendrimers, as long as the molecules are highly charged and the solutions of low ionic strength, the observed behavior is remarkably similar.

The critical issue for future studies is to define the mechanism leading to formation of multichain domains. The preponderance of evidence suggests that an effective, attractive interpolyion interaction must exist, and this hypothesis has sparked renewed interest with some exciting results and new predictions.[21,54−60] It is clear that the role of comprehensive experiments becomes even more critical as the questions raised spark new models which require examination.

## Conclusion

From this study, we demonstrate that the steep upturn at low $q$ values, observed previously by several groups in small-angle scattering measurements on a variety of systems, is not an artifact or an insignificant contribution to the overall scattering profile of low ionic strength polyelectrolyte solutions. Furthermore, the upturn, which reflects long-wavelength concentration fluctuations, is consistent with static light scattering and dynamic light scattering performed on the same solutions. Debye function fits to the SLS data reveal apparent $R_g$ values of about 90 nm over a decade in concentration range. We interpret these structures as multichain domains which are present even in dilute solutions of polyelectrolytes. In these same solutions, a shorter length scale is evident from the peak in SANS at finite $q$ and the fast mode in DLS. We interpret the peak as evidence of a network structure with short-range order existing within domains. The DLS fast mode is attributed to electrodynamic coupling of chain segments with fast moving, low-molecular-weight counterions.

**Acknowledgment.** We are grateful to Dr. Giovanni Nisato, Dr. Charles Han, and Dr. Jack F. Douglas for their helpful discussions and critical reading of the manuscript.

## References and Notes

(1) Tanford, C. *Physical Chemistry of Macromolecules*; Wiley: New York, 1965.
(2) *Polyelectrolytes: Science and Technology*; Hara, M., Ed.; Marcel Dekker: New York, 1993.
(3) *Macro-ion Characterization*; Schmitz, K., Ed.; American Chemical Society: Washington, DC, 1994.
(4) Dautzenberg, H.; Jaeger, W.; Kötz, J.; Phillip, B.; Seidel, Ch.; Stscherbina, D. *Polyelectrolytes: Formation, Characterization and Application*; Hanser/Gardner: Cincinnati, OH, 1994.
(5) Barrat, J. L.; Joanny, J. F. In *Polymeric Systems*; Prigogine, I., Rice, S. A., Eds.; John Wiley and Sons: New York, 1996.
(6) Lin, S. C.; Lee, W. I.; Schurr, J. M. *Biopolymers* **1978**, *17*, 1041.
(7) Mathiez, P.; Mouttet, C.; Weisbuch, G. *Biopolymers* **1981**, *20*, 2381.
(8) Schmitz, K. S.; Lu, M.; Gauntt, J. *J. Chem. Phys.* **1983**, *78*, 5059.
(9) Drifford, M.; Dalbiez, J. P. *Biopolymers* **1985**, *24*, 1501.
(10) Borsali, R.; Nguyen, H.; Pecora, R. *Macromolecules* **1998**, *31*, 1548.
(11) Koene, R. S.; Mandel, M. *Macromolecules* **1983**, *16*, 973.
(12) Sedlák, M.; Konák, C.; Stepánek, P.; Jakes, J. *Polymer* **1987,** *28*, 873.
(13) Schmitz, K. S.; Yu, J. *Macromolecules* **1988**, *21*, 484.
(14) Schmidt, M. *Makromol. Chem., Rapid Commun.* **1989**, *10*, 89.
(15) Förster, S.; Schmidt, M.; Antonietti, M. *Polymer* **1990**, *31*, 781.
(16) Sedlák, M.; Amis, E. J. *J. Chem. Phys.* **1992**, *96*, 817.
(17) Ermi, B. D.; Amis, E. J. *Macromolecules* **1996**, *29*, 2703.
(18) Topp, A.; Belkoura, L.; Woermann, D. *Macromolecules* **1996**, *29*, 5392.

(19) Nerling, W.; Nordmeir, E. *Polym. J.* **1997**, *29*, 795.
(20) Valachovic, D. E.; Amis, E. J.; Tomalia, D. A. *ACS Polym. Prepr.* **1995**, *36* (1), 373.
(21) Muthukumar, M. *J. Chem. Phys.* **1997**, *107*, 2619.
(22) Rinaudo, M.; Domard, A. *J. Polym. Sci., Polym. Lett. Edn.* **1979**, *15*, 411.
(23) Matsuoka, H.; Ise, N.; Okubo, T.; Kunugi, S.; Tomiyama, H.; Yoshikawa, Y. *J. Chem. Phys.* **1985**, *83*, 378.
(24) Milas, M.; Rinaudo, M.; Duplessix, R.; Borsali, R.; Lindner, P. *Macromolecules* **1995**, *28*, 3199.
(25) Cotton, J. P.; Moan, M. *J. Phys. Fr.* **1976**, *37*, 75.
(26) Moan, M. *J. Appl. Crystallogr.* **1978**, *11*, 519.
(27) Nierlich, M.; Williams, C. E.; Boué, F.; Daoud, M.; Farnoux, B.; Jannick, G.; Picot, C.; Moan, M.; Wolff, C.; Rinaudo, M.; de Gennes, P. G. *J. Phys. Fr.* **1979**, *40*, 701.
(28) Matsuoka, H.; Schwahn, D.; Ise, N. *Macromolecules* **1991**, *24*, 4227.
(29) Ise, N.; Okubo, T.; Kunugi, S.; Matsuoka, H.; Yamamoto, K.; Ishii, Y. *J. Chem. Phys.* **1984**, *81*, 3294.
(30) Moussaid, A.; Schosseler, F.; Munch, J. P.; Candau, S. J. *J. Phys. II Fr.* **1993**, *3*, 573.
(31) Boué, F.; Cotton, J. P.; Lapp, A.; Jannick, G. *J. Chem. Phys.* **1994**, *101*, 2562.
(32) Shibayama, M.; Tanaka, T. *J. Chem. Phys.* **1995**, *102*, 9392.
(33) Essafi, W.; Lafuma, F.; Williams, C. E. *J. Phys. II Fr.* **1995**, *5*, 1269.
(34) Essafi, W.; Lafuma, F.; Williams, C. E. In *Macro-ion Characterization*; Schmitz, K., Ed.; American Chemical Society: Washington, DC, 1994.
(35) Ermi, B. D.; Amis, E. J. *Marcomolecules* **1997**, *30*, 6937.
(36) Bauer, B. J.; Briber, R. M.; Hammouda, B.; Tomalia, D. A. *ACS PMSE Prepr.* **1992**, *67*, 430.
(37) Valachovic, D. E.; Bauer, B. J.; Amis, E. J.; Tomalia, D. A. *ACS PMSE Prepr.* **1997**, *77*, 230.
(38) Valachovic, D. E. Ph.D. Dissertation, University of Southern California, 1997.
(39) Hayter, J. B.; Jannick, G.; Brochard-Wyart, F.; de Gennes, P. G. *J. Phys.* **1980**, *41*, L451.
(40) Koyama, R. *Macromolecules* **1984**, *17*, 1594.
(41) de Gennes, P. G.; Pincus, P.; Velasco, R. M.; Brochard, F. *J. Phys. Fr.* **1976**, *37*, 1461.
(42) Pfeuty, P. J. *J. Phys. Fr. Coll. C2* **1978**, *39*, 149.
(43) Dobrynin, A. V.; Colby, R. H.; Rubinstein, M. *Macromolecules* **1995**, *28*, 1859.
(44) Yamaguchi, M.; Yamaguchi, Y.; Masushita, Y.; Noda, I. *Polym. J. (Jpn.)* **1990**, *22*, 1107.
(45) According to ISO 31-8, the term "molecular weight" has been replaced with "relative molecular mass", symbol $M_r$. Thus, if this nomenclature and notation were followed in this publication, one would write $M_{r,n}$, instead of the historically conventional $M_n$ for the number-average molecular weight, with similar changes for $M_w$, $M_z$, and $M_v$, and it would be called the "number-average relative molecular mass". The conventional notation, rather than the ISO notation, has been employed for this publication.
(46) Certain commercial material and equipment are identified in this publication in order to specify adequately the experimental procedure. In no case does such identification imply recommendation by the National Institute of Standards and Technology, nor does it imply that the material or equipment identified is necessarily the best available for this purpose.
(47) Provencher, S. W. *Comput. Phys. Commun.* **1982**, *27*, 213.
(48) Provencher, S. W. *Comput. Phys. Commun.* **1982**, *27*, 229.
(49) All uncertainty values reported in this publication are for one standard deviation.
(50) Kerker, M. *The Scattering of Light and Other Electromagnetic Radiation*; Academic Press: New York, 1969.
(51) Higgins, J.; Benoit, H. *Polymers and Neutron Scattering*; Oxford University Press: New York, 1994.
(52) Borue, V. Y.; Erukhimovich, I. Y. *Macromolecules* **1988**, *21*, 3240.
(53) Joanny, J. F.; Leibler, L. *J. Phys. Fr.* **1990**, *51*, 545.
(54) Muthukumar, M. *J. Chem. Phys.* **1996**, *105*, 5183.
(55) Ray, J.; Manning, G. S. *Langmuir* **1994**, *10*, 2450.
(56) Ise, N.; Yoshida, H. *Acc. Chem. Res.* **1996**, *29*, 5.
(57) Schmitz, K. S. *Acc. Chem. Res.* **1996**, *29*, 7.
(58) Grønbech-Jensen, N.; Mashl, R. J.; Bruinsma, R. F.; Gelbart, W. M. *Phys. Rev. Lett.*, **1997**, *78*, 2477.
(59) Ha, B. Y.; Liu, A. J. *Phys. Rev. Lett.* **1997**, *79*, 1289.
(60) Schmitz, K. S. *Langmuir* **1997**, *13*, 5849.
(61) Förster, S.; Schmidt, M. *Adv. Polym. Sci.* **1995**, *120*, 51.

MA980579+